small
NANO MICRO

Large Dynamic Range Digital Nanodot Gradients of Biomolecules Made by Low-Cost Nanocontact Printing for Cell Haptotaxis

*Sébastien G. Ricoult, Mateu Pla-Roca, Roozbeh Safavieh, G. Monserratt Lopez-Ayon, Peter Grütter, Timothy E. Kennedy, and David Juncker**

***A** novel method is introduced for ultrahigh throughput and ultralow cost patterning of biomolecules with nanometer resolution and novel 2D digital nanodot gradients (DNGs) with mathematically defined slopes are created. The technique is based on lift-off nanocontact printing while using high-resolution photopolymer stamps that are rapidly produced at a low cost through double replication from Si originals. Printed patterns with 100 nm features are shown. DNGs with varying spacing between the dots and a record dynamic range of 4400 are produced; 64 unique DNGs, each with hundreds of thousands of dots, are inked and printed in 5.5 min. The adhesive response and haptotaxis of C2C12 myoblast cells on DNGs demonstrated their biofunctionality. The great flexibility in pattern design, the massive parallel ability, the ultra low cost, and the extreme ease of polymer lift-off nanocontact printing will facilitate its use for various biological and medical applications.*

1. Introduction

Patterning of biomolecules and notably proteins on surfaces has been critical to advances in microarrays, biosensors, and cell biology.[1,2] Proteins are the main effectors in cells and are important for bioanalysis, but they are labile and cannot be exposed to harsh conditions due to risks of denaturation which results in a loss in biological activity. Patterning of proteins cannot be done by photolithography, and alternative methods, such as Inkjet printing, are now well established, but the resolution is typically limited to 100 μm.[3] Interestingly, proteins can be patterned by microcontact printing by first inking a soft stamp by incubating it in a protein solution, briefly drying it, and placing it onto a target substrate so as to effect the transfer of proteins from the stamp to the substrate. However, conventional microcontact printing suffers from a number of limitations and it is for example difficult to achieve resolution <1 μm or large spacing in the pattern due to the risk, and occurrence, of collapse of the soft, elastomeric stamps.[4] Alternative methods with greater flexibility such as dip pen lithography were developed,[5] but they are slow and cumbersome. Recently, parallel dip-pen patterning was introduced,[6] which helped improve the throughput, however it does not allow for direct control of the tips and is thus limited to the replication of patterns no larger than the spacing between two tips. More recently, high resolution Si stencil was introduced to make nanoarrays,[7] but so far only small arrays with each only one ink were made, and the stencils are fragile and costly to make.

S. G. Ricoult, Dr. M. Pla-Roca, R. Safavieh, Prof. D. Juncker
Department of Biomedical Engineering
McGill University and Génome Québec Innovation Centre
McGill University
740 Dr. Penfield Avenue
Montréal, Québec H3A 0G1, Canada
Fax: (+)1 (514) 398 1790; Webpage: http://wikisites.mcgill.ca/djgroup/
E-mail: david.juncker@mcgill.ca

S. G. Ricoult, Prof. T. E. Kennedy, Prof. D. Juncker
Department of Neuroscience
McGill University
3801 University Avenue, Montréal
Québec H3A 0G1, Canada

G. M. Lopez-Ayon, Prof. P. Grütter
Center for the Physics of Materials and the Department of Physics
McGill University
Montréal, Québec H3A 2T8, Canada

DOI: 10.1002/smll.201202915

A modified microcontact printing method called lift-off printing has increased resolution and overcome the limitations of aspect ratio and stamp collapse.[8] For proteins, lift-off printing has been conducted by pressing a hard, Si "master" stamp containing recesses against a flat stamp coated with protein, thus lifting-off proteins in the contact areas, but leaving untouched the ones located below a recess. These proteins can then be transferred onto a glass surface by printing the flat stamp without risk of collapse. Recently, the use of PDMS stamps has been introduced for reactive lift-off of thiols on gold,[9] but only Si stamps have been used for protein lift-off to date. Coyer et al. used lift-off printing to produce digital gradients by varying the spacing of dots along one axis perpendicular to the gradient direction from 1 μm to 64 μm, corresponding to a 63 fold change, which expressed in log 10 corresponds to a dynamic range of 1.8 orders of magnitude (OM).[7,10] However, Si lift-off masters are expensive to make, and their lifetime is limited as they get contaminated by each print, and thus only a restricted number of patterns can be produced, keeping the overall costs of patterning high and limiting their usefulness.

Here, we introduce two significant advances. Firstly, we use photo-crosslinked polymer masters for lift-off nanocontact printing of proteins and peptides with feature sizes down to 100 nm. The polymer masters are double-replicated from a Si master where at each step multiple copies can be made, to produce a very large number of prints exceeding 400 from a single Si nanopattern. Secondly, we present a novel DNG that while being unidirectional varies in two-dimension and has the greatest dynamic range of any single gradient produced to date to our knowledge, and which could be further expanded. The response and haptotaxis of C2C12 muscle cells to both peptide and protein DNGs was established.

2. Results and Discussion

DNGs, each between 200 and 400 μm long depending on the slope, and 400 μm wide, were designed using 200 nm wide dots with varying spacing between the dots. To increase the dynamic range of the gradient, the spacing of the dots was changed in two dimensions, both parallel and perpendicular to the gradient direction. We developed an algorithm to create such patterns while producing a continuous gradient. The DNGs were formed by subdividing the gradient into "boxes" each 400 μm long and with a height ~8 μm (depending on the gradient and the position). The spacing of nanodots within one box is constant, while in each box it was adjusted to depend on the position of the box so as to match the density corresponding to the position in the gradient. **Figure 1** shows one such gradient composed of 53 rectangles that are 400 μm long and 7.5 μm wide while the center-to-center spacing of the dots in each rectangle varies from 0.3 μm to 4.83 μm along both X and Y. Here, the spacing d of the dots within each box follows the power law $d = 3\mu m \times (\text{box number})^{\sqrt{2}/2}$. The dynamic range of this DNG is 259 or 2.4 OM. Linear, exponential, or power-law gradients can be produced by using the appropriate function to calculate the dot spacing in each box. The DNG with the highest dynamic range

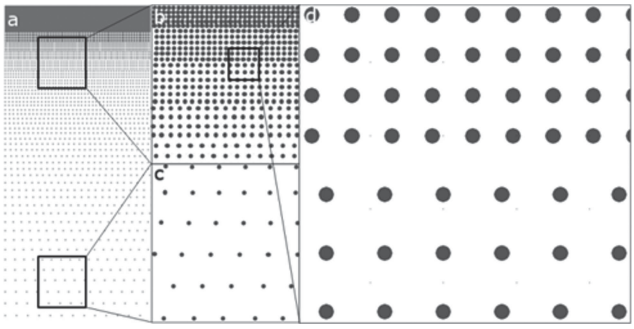

Figure 1. DNG design. (a) Excerpt of a DNG made up of 88,521 200 nm dots with center-to-center spacing decreasing from 4.85 μm to 300 nm. The gradient is composed of 53 rectangular boxes $7.5 \times 400\ \mu m^2$ in size with an array of dots of constant spacing in both X and Y directions within each box. (b,c) Close-up views from the high and low density regions at the top and bottom of the gradient, respectively. (d) Close-up view of a section of the gradient showing 200 nm dots with a center-to-center spacing of 792 nm for the top 4 rows and 926 nm for the bottom 3 rows.

extended from full coverage at one end to one 200 nm dot ($= 0.0314\ \mu m^2$) within an area of $11.75 \times 11.75 = 138\ \mu m^2$ at the other end, corresponding to a dynamic range of 4400, or 3.6 OM. This constitutes the highest dynamic range reported to date for a single continuous surface gradient to the best of our knowledge, while the maximal spacing is relevant to cell migration. Indeed, the maximal spacing was limited to ~12 μm between the dots so that a cell would be in contact with at least one dot. Larger spacing could easily be produced if desired. By changing the various parameters such as minimal and maximal spacing and the slope, 64 different gradients were designed and collectively occupied an area of $5.4 \times 5.8\ mm^2$.

An accurate polymer copy of the Si wafer with the etched nanopatterns was obtained after double replication using poly(dimethylsiloxane) (PDMS) and a UV sensitive photopolymer (Norland Optical Adhesive 63 (NOA)), (**Figure 2**).[11] The details of the process are provided in the accompanying methods. Scanning electron microscopy (SEM) and atomic force microscopy (AFM) images of the original Si master, the intermediate, and the final replicate, show a high fidelity (Figure S1). In addition to the 200 nm dots, we also produced stamps with 100 nm features and successfully printed them, Figure S2. However, for cells to recognize the nanodots and efficiently form focal adhesions, it has been shown that protein aggregates less than 200 nm large fail to elicit a cell response,[12] thus 200 nm dots were used for the DNGs.

The throughput and cost of nanocontact printing benefit from multiple replications and the massive parallelism of printing. To test the possibility for making multiple copies, the Si wafer was replicated over 20 times into PDMS, and the 20th copy in turn replicated into NOA more than 20 times (Figure S2). We believe that well over 400 replicates could be made but did not pursue the experiment further. It takes ~1 min for PDMS to NOA replication, allowing tens of NOA copies to be rapidly produced. All 64 gradients which comprise 7.6×10^6 dots can be printed in parallel in a 5 s lift-off

small 2013,
DOI: 10.1002/smll.201202915

NANO MICRO small

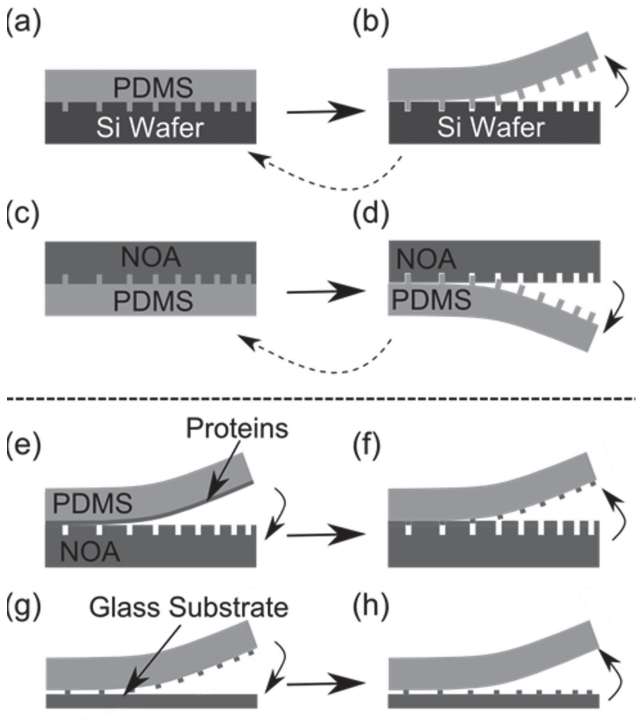

Figure 2. Schematic of the double replication process to make polymer replicas and their subsequent use as masters for lift-off nanocontact printing. (a) A Si wafer with a DNG of 200 nm holes is covered with PDMS, which is cured, and (b) separated from the wafer. The PDMS is in turn covered with a photo-sensitive polymer (NOA), exposed to light, and (d) the NOA replica separated. A planar PDMS stamp is incubated with a protein solution, blown dry, and (e) quickly brought into contact with a NOA replica that was plasma activated, and separated to lift-off proteins in the contact areas. (g) The flat PDMS stamp is then printed onto a glass slide and (h) separated, producing a DNG of protein on the slide.

step. The material cost of an NOA replica with the 64 gradients (0.8 mL) is only 0.13 USD. We paid 450 USD for the Si wafer patterned by e-beam. The material cost of a PDMS replica (50 mL) is ~6 USD. The combined material cost for each replica with 64 DNGs, assuming 400 copies, is thus 1.55 USD, or 2.4 cents per gradient. Whereas until now production of arbitrary nanopatterns has been very cost and time intensive, DNGs can be produced with great ease and at low cost. Indeed, once the double-replication nanopatterning procedure had been optimized, the time, efforts and cost of DNG production were negligible compared to the needs of cell culture, imaging and data analysis.

A solution of arginine-glycine-aspartic acid (RGD) peptide mixed with fluorescently-labelled immunoglobulin G (IgGs) for visualization was used as "ink" for the printing process, Figure 1e,f. Following optimization, high yields were achieved for protein nanopatterning with a minimal number of defects, **Figure 3**a. These results indicate that NOA, and by extension other hard polymeric materials, may serve as efficient and reliable masters for lift-off nanocontact printing of biomolecules. Defects were rare and could be attributed to dust particles that adsorbed to the PDMS during replication, and might be further reduced by working in a clean room. Whereas Si masters may be used repeatedly for lift-off

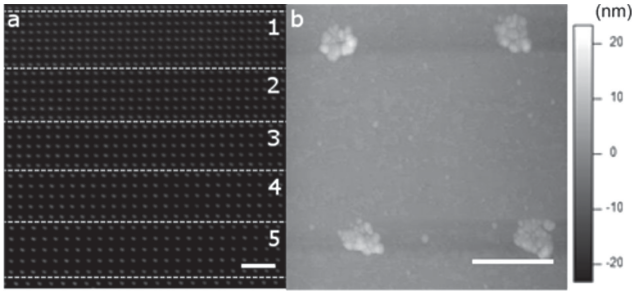

Figure 3. Confocal fluorescence microscope and AFM images of a DNG patterned by lift-off nanocontact printing. (a) Grids of 200 nm dots of a peptide-protein "ink" made of RGD peptide mixed 1:1 by mass with a fluorescently labeled antibody. The image shows 5 rectangular boxes of the DNG with a grid size of 1052 nm, 1171 nm, 1286 nm, 1397 nm and 1504 nm for boxes labeled 1–5, respectively. (b) AFM image of box 1. The image reveals the rugged shape of individual dots and features within the dot that delineates individual IgG proteins. The height of the dots was measured to be 5 nm on average. Scale bar for (a) is 3 μm and (b) 500 nm.

printing,[10] recycling NOA stamps was not effective as the second print displayed multiple defects. It may be possible to overcome this limitation using more harsh cleaning procedures, but it was not pursued here given that NOA masters were inexpensive and plentiful.

The nanodots were characterized using an AFM operated in tapping mode. The nanodots have rugged edges due to the globular nature of the proteins (Figure 3b). The diameter of the dots was established using an image recognition algorithm ("analyze particle" function in Image J, NIH) for 16 dots and found to be 210 nm ± 18 nm, thus closely matching the original design of 200 nm. Variability in dot size may be contributed by minor imprecision during replication, the finite size of proteins which may only partially contact the lift-off stamp at the edges and thus add to the variability, as well as lateral interactions between proteins that may entrain or restrain adjacent proteins. Dot size is however not expected to vary with the change in gradient density since proteins are adsorbed evenly on a flat surface and lifted off, and hence the pattern density is not apparent during the incubation and lift-off steps.

To test the bioactivity of the printed proteins and the utility of DNGs for cell biology, we first studied cellular migration on DNGs of RGD peptides. The amino acid sequence RGD is a binding site for transmembrane integrins that form a molecular link between the ECM and the cytoskeleton and is found in ECM proteins such as fibronectin[13] and laminin.[14] Surface gradients of laminin guide the migration of rat hippocampal neurons,[15] embryonic Xenopus spinal neurons[16] and rat intestinal IEC-6 cells,[17] while RGD peptides have been demonstrated to orient fibroblast migration.[18]

DNGs of RGD peptides were patterned by lift-off nanocontact printing as described above. Next, a solution of 75% poly-L-lysine grafted with polyethylene glycol (PLL-g-PEG)[19,20] and 25% Poly-D-lysine (PDL) by volume was applied to the coverslip to backfill the surface with an appropriate background for maximizing the cell response to the

DOI: 10.1002/smll.201202915

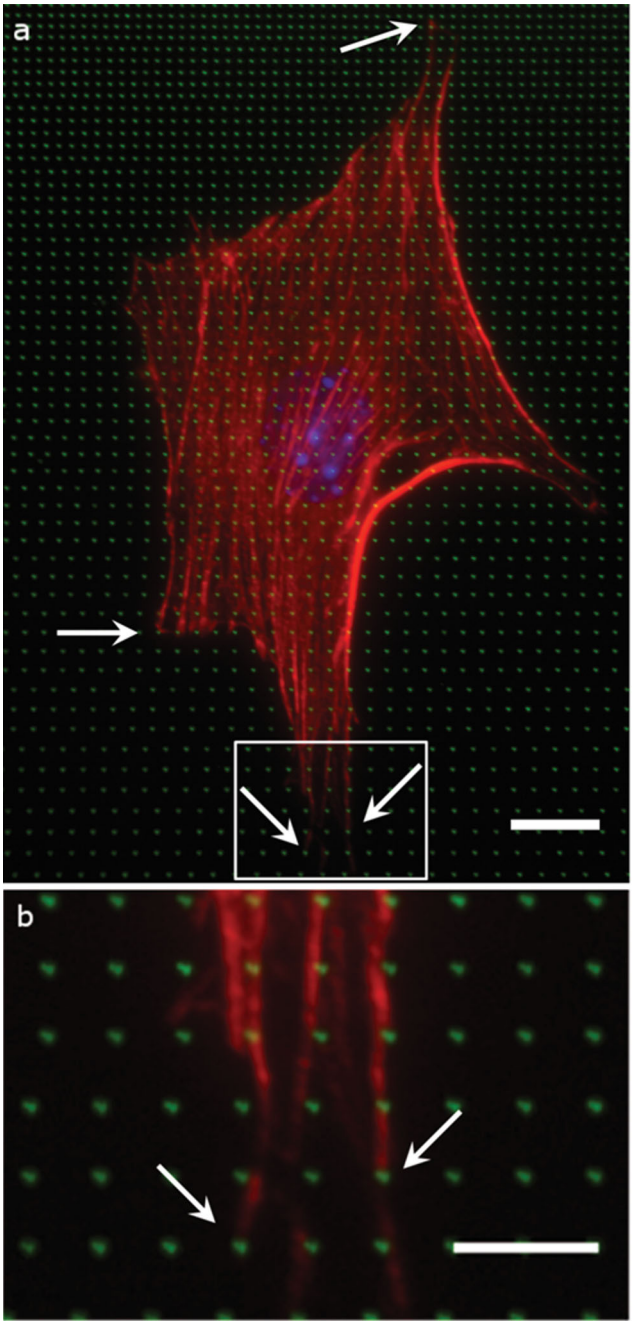

Figure 4. C2C12 myoblast cell on a DNG of RGD peptides. (a) Fluorescent micrograph of a DNG or RGD peptides mixed with fluorescent IgG (green dots) and a C2C12 cell grown for 18 h, fixed and stained to reveal actin filaments (red) and the cell nucleus (blue). (b) Close-up of the frame in (a) showing that actin filaments align with the nanodot patterns. Arrows indicate areas where cell shape or structures strikingly coincide with the nanodot pattern. Scale bar for (a) is 10 µm and (b) 5 µm.

DNG (the development of this method and the rationale will be discussed in detail elsewhere). C2C12 myoblast cells were seeded on the coverslip and grown for 18 h. The response of C2C12 cells to DNGs was assessed by fluorescence microscopy (**Figure 4**, Figure S4). C2C12 cells adhered to the surface, extended filopodia, and migrated along the gradient. Negative control experiments were performed by replacing the RGD peptide with Immunoglobulin G (IgG) proteins

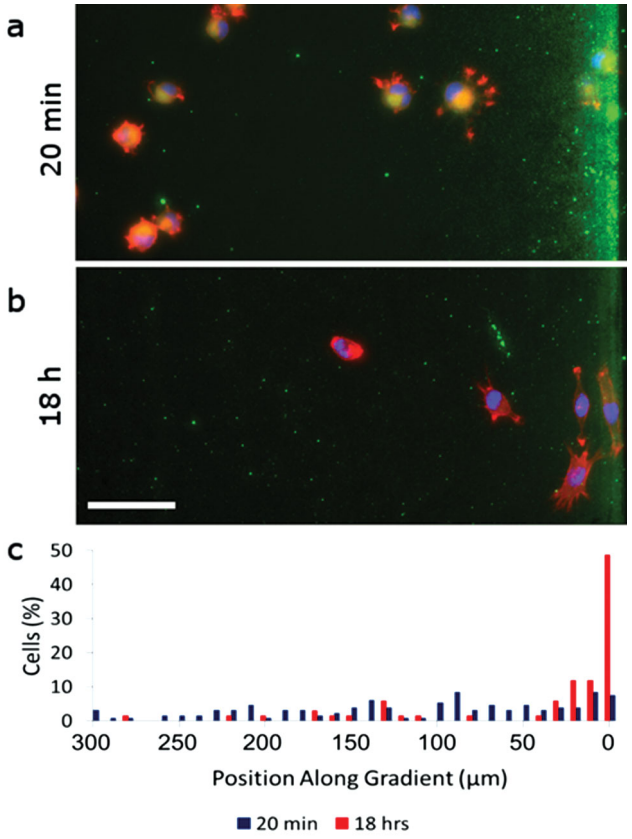

Figure 5. C2C12 myoblast migration on a netrin-1 DNG. Netrin-1 was mixed with fluorescent IgG (9:1 ratio) for visualization (green dots) and the C2C12 cells were fixed and stained to reveal actin filaments (red) and the cell nucleus (blue). C2C12 cells were seeded on the coverslip with the DNGs and one set fixed and imaged after (a) 20 min and the other after (b) 18 h. (c) Distribution of cells on 30 DNGs 20 min and 18 h after seeding. Over time, cells accumulate at the top of the gradient where the density of dots is the highest. Scale bar is 65 µm.

and lead to a loss of cell adhesion (Figure S5), thus confirming that cells specifically responded to the peptide. In order to show the generality of the method in terms of both patterning and applications, the protein netrin-1 was patterned as DNG to study cell haptotaxis[21] that is a chemoattractant for C2C12 myoblasts.[22] Cells were imaged 20 min after seeding immediately after attachment to the substrate and after 18 h. Whereas cells were initially distributed over the entire netrin-1 DNG, they were subsequently preferentially located in the high density area, **Figure 5**a,b. Cell haptotaxis on DNGs was quantified by recording cell distribution on 30 gradients in 8 separate experiments upon seeding and after 18 h of incubation, Figure 5c. Cells were distributed almost equally throughout the gradient initially, while 50% of the cells were localized within 30 µm of the highest density edge of the netrin-1 gradients. There were n = 133, cells on the netrin-1 gradients at the beginning, and n = 68 at the end of the experiment. Whereas we observed cells from the center of the gradient migrate in the direction of higher density, cells at the lower end migrated in all directions and many left the gradient into the relatively vast surrounding space. Additional experiments with live imaging to quantify cell

small 2013,
DOI: 10.1002/smll.201202915

NANO MICRO small

responses to various gradient slopes and as a function of the initial position are in progress, but are beyond the scope of this manuscript and will be reported elsewhere. On control gradients composed of patterned IgG, the cells appeared randomly distributed at the beginning. At the end, relatively few cells remained on the gradients, but were randomly scattered throughout the gradient (Figure S6).

3. Conclusion

In conclusion, we have developed a novel versatile, ultra low cost and massively parallel nanocontact printing process that can produce 100 nm features. The polymer masters are made by double replication of Si wafers and features replicated with ~30 nm accuracy, indicating that much higher resolution is feasible.[11] We developed protocols for printing DNGs of proteins covering large areas at a material cost of a few cents per gradient. The 7.6×10^6 dots of all gradients were printed in a 5 s lift-off step at a rate of 1.3×10^5 dots s^{-1}, which makes it one of the fastest nanopatterning methods; during the course of the optimization we estimate that we produced over 900 prints. The surface gradients presented here span a dynamic range of up to 3.6 OM, which is the highest reported to date and represents an 80 fold increase over previous digital gradients,[10] and represents the maximum for cell migration studies given the upper and lower bounds. Smaller patterns and higher resolutions are readily achievable, and the dynamic range may thus be further expanded if desired. The biological relevance of DNGs was established by observing C2C12 mouse myoblasts spreading and migrating on DNGs of RGD peptides and netrin-1 protein, respectively. DNGs will be useful for studying how cells, including lymphocytes and neurons, respond to both attractive and repellent gradients while monitoring their response in real time. DNGs may also be combined with microfluidic devices[16] or microfluidic probes[23] to apply a combination of cues to cells. The implementation of DNGs for repulsive assays will be technically more challenging since cells will need to attach to the surface, and be precisely positioned at the high density portion of the gradient to reveal directed motion away from the cue. The low cost and ease-of-use of polymer nanocontact lift-off printing will allow its widespread adoption, including in laboratories without access to nanofabrication facilities, and routine use for a variety of biological and medical applications.

4. Experimental Section

Preparation of Lift-off Stamps: A computer generated design of the DNGs with 200 nm dots was created in Clewin Pro 4.0 (Wieweb software, Hengelo, Netherlands). A 4" silicon wafer was coated with PMMA resist and the dot arrays patterned by electron beam lithography (VB6 UHR EWF, Vistec), followed by 100 nm reactive ion etching (System100 ICP380, Plasmalab) into the Si. After cleaning, the wafer was coated with an anti-adhesive layer by exposing it to perfluorooctyltriethoxysilane (Sigma-Aldrich, Oakville, ON, Canada) in vapor phase in a desiccator. An accurate polymer copy of the Si wafer was obtained after double replication using poly(dimethylsiloxane) (PDMS) and a UV sensitive polyurethane (Figure 1).[24] Firstly, a ~6 mm layer of 1:10 PDMS (Dow Corning, Corning, NY, USA) was poured on the wafer inside a Petri dish, followed by removal of bubbles under vacuum in a desiccator for 10 min. Next, the PDMS was cured in an oven for 24 h at 60 °C (VWR, Montreal, QC, Canada), and then peeled off of the wafer. To remove un-crosslinked extractables, the PDMS replica was bathed in 70% ethanol for 24 h and then baked at 60 °C for 4 h. Secondly, a large drop of UV sensitive polyurethane (Norland Optical Adhesive 63 (NOA); Norland Products, Cranbury, NJ) was poured on the PDMS and cured by exposing it to 600 W of UV light (Uvitron International, Inc., West Springfield, MA) for 50 s. The PDMS was then peeled off, thus yielding an NOA replica of the Si pattern.

Lift-off Microcontact Printing: A flat PDMS stamp cured against a Si wafer treated with a perfluorooctyltriethoxysilane anti-adhesive layer was used for lift-off nanocontact printing against the NOA replicas—now serving as master—with 200 nm holes. Following removal of the extractables as described above, the flat PDMS stamp was inked with a 10 µL drop of phosphate buffered saline solution (PBS) containing either 25 µg/mL of the Arginine-Glycine-Aspartic acid (RGD) peptide (CHI Scientific Inc., Maynard, MA) or 25 µg/mL of netrin-1 (12.5 µg/mL, produced and purified as described,[25,26]) both mixed with 25 µg/mL of chicken immunoglobulin G (IgG) conjugated to Alexa Fluor 488 (Invitrogen, Burlington, ON, Canada) for visualization or IgG alone for the negative control experiments. A plasma activated hydrophilic coverslip was then placed on the drop to spread the solution evenly on the surface of the hydrophobic PDMS stamp during a 5 min incubation period. After rinsing with PBS and double distilled water for 30 s, the inked stamps were briefly dried under a stream of N2 and immediately brought into contact with a plasma activated (Plasmaline 415, Tegal, Petaluma, CA, USA) NOA master for 5 s. The PDMS was separated and the proteins in the contact areas were transferred to the NOA, while the remaining proteins transferred to the final substrate by printing the PDMS stamp for 5 s onto a plasma activated glass coverslip.

Cell Culture: Patterned RGD DNGs used in our experiments were backfilled by coating the areas between the nanodots with a solution composed of 75% poly-L-lysine (PLL) conjugated with polyethylene glycol (PEG) (PLL(20)-g[3.5]-PEG[2], Surface Solutions, Grande Prairie, AB, Canada)[27,28] and 25% poly-D-lysine (PDL, 70-150 kDa, Sigma-Aldrich, Oakville, ON, Canada) by volume, which was done by incubating the coverslip with the mixture at a concentration of 10 µg/ml. We seeded 50,000 C2C12 myoblast cells per coverslip and grew them on the patterned substrate for 18 h at 37 °C in 5% CO2 in high glucose DMEM, 10% Fetal Bovine Serum and 1% Penicillin/Streptomycin (all from Invitrogen) growth media. Cells were fixed after 18 h of growth with 4% paraformaldehyde for 1 min, permeabilized with triton-X 100 for 5 min and blocked with Horse Serum for 1 h. C2C12 myoblasts were labeled with phalloidin conjugated to Alexa Fluor 555 (1:250, Invitrogen, Burlington, ON, Canada) and with Hoechst stain (1:10,000, Invitrogen, Burlington, ON, Canada). Protein dots were colocalized with a secondary chicken anti-goat antibody conjugated to Alexa Fluor 488 (polyclonal, 1:20, Invitrogen, Burlington, ON, Canada).

Imaging: Images of the original Si master, and the intermediate and final replicates were collected using scanning electron microscopy (SEM, Hitachi, Mississauga, ON) and Atomic Force Microscopy (AFM, Asylum Research, Santa Barbara, CA). DNGs of

DOI: 10.1002/smll.201202915

fluorescent IgG and C2C12 myoblasts grown on the DNGs were imaged by fluorescence microscopy (TE2000, Nikon). The location of fixed cells was determined by the center of the nucleus of the stained cells. Their position on the gradient was measured from the edge of the gradient at the highest density.

Supporting Information

Supporting Information is available from the Wiley Online Library or from the author.

Acknowledgements

The authors wish to thank Yannick Devaud, Levon Atoyan and Natalia Tansky for their contributions to nanocontact printing, Tohid Fatanat Didar for providing RGD peptides and Prof. Craig Mandato for providing C2C12 cells. We acknowledge support from CIHR (Regenerative and Nanomedicine grant), the Canadian Foundation for Innovation and the McGill Nanotools Microfabrication Laboratory (funded by CFI and McGill University). SGR was supported by a Jeanne Timmins Costello Studentship, the NSERC-Create Integrated Sensor System Program and the Neuroengineering program funded by CIHR and The Molson Foundation. TEK is a Killam Foundation Scholar and holds a Chercheur National award from the Fonds de la Recherche en Santé du Québec. DJ holds a Canada Research Chair.

[1] A. Sassolas, B. D. Leca-Bouvier, L. J. Blum, *Chem. Rev.* **2007**, *108*, 109–139.
[2] A. S. Blawas, W. M. Reichert, *Biomaterials* **1998**, *19*, 595–609.
[3] J. T. Delaney, P. J. Smith, U. S. Schubert, *Soft Matter* **2009**, *5*, 4866–4877.
[4] A. Perl, D. N. Reinhoudt, J. Huskens, *Adv Mater* **2009**, *21*, 2257–2268.
[5] R. D. Piner, J. Zhu, F. Xu, S. Hong, C. A. Mirkin, *Science* **1999**, *283*, 661–663.
[6] Z. Zheng, W. L. Daniel, L. R. Giam, F. Huo, A. J. Senesi, G. Zheng, C. A. Mirkin, *Angew. Chem. Int. Ed.* **2009**, *48*, 7626–7629.
[7] M. Huang, B. C. Galarreta, A. Artar, R. Adato, S. Aksu, H. Altug, *Nano Lett.* **2012**, *12*, 4817–4822.
[8] J. Renault, A. Bernard, D. Juncker, B. Michel, H. Bosshard, E. Delamarche, *Angew. Chem.* **2002**, *114*, 2426–2429.
[9] W.-S. Liao, S. Cheunkar, H. H. Cao, H. R. Bednar, P. S. Weiss, A. M. Andrews, *Science* **2012**, *337*, 1517–1521.
[10] S. R. Coyer, A. J. Garcia, E. Delamarche, *Angew. Chem. Int. Ed.* **2007**, *46*, 6837–6840.
[11] Y. N. Xia, J. J. McClelland, R. Gupta, D. Qin, X. M. Zhao, L. L. Sohn, R. J. Celotta, G. M. Whitesides, *Adv. Mater.* **1997**, *9*, 147–149.
[12] B. Geiger, J. P. Spatz, A. D. Bershadsky, *Nat. Rev. Mol. Cell Bio.* **2009**, *10*, 21–33.
[13] K. Linask, J. Lash, *Dev. Biol.* **1986**, *114*, 87–101.
[14] J. McCarthy, S. Palm, L. Furcht, *J. Cell Biol.* **1983**, *97*, 772.
[15] S. Dertinger, X. Jiang, Z. Li, V. Murthy, G. Whitesides, *Proc. Natl. Acad. Sci. USA* **2002**, *99*, 12542.
[16] C. J. Wang, X. Li, B. Lin, S. Shim, G. L. Ming, A. Levchenko, *Lab Chip* **2008**, *8*, 227–237.
[17] R. C. Gunawan, J. Silvestre, H. R. Gaskins, P. J. A. Kenis, D. E. Leckband, *Langmuir* **2006**, *22*, 4250–4258.
[18] C. E. Kang, E. J. Gemeinhart, R. A. Gemeinhart, *J. Biomed. Mater. Res. A* **2004**, *71A*, 403–411.
[19] V. Saravia, S. Küpcü, M. Nolte, C. Huber, D. Pum, A. Fery, U. Sleytr, J. Toca-Herrera, *J. Biotechnol.* **2007**, *130*, 247–252.
[20] W. Senaratne, P. Sengupta, C. Harnett, H. Craighead, B. Baird, C. Ober, *NanoBioTechnology* **2005**, *1*, 23–33.
[21] K. L. W. Sun, J. P. Correia, T. E. Kennedy, *Development* **2011**, *138*, 2153–2169.
[22] J.-S. Kang, M.-J. Yi, W. Zhang, J. L. Feinleib, F. Cole, R. S. Krauss, *J. Cell Biol.* **2004**, *167*, 493–504.
[23] M. A. Qasaimeh, S. G. Ricoult, D. Juncker, *Lab Chip* **2013**, 13, 40–50.
[24] Y. N. Xia, J. J. McClelland, R. Gupta, D. Qin, X. M. Zhao, L. L. Sohn, R. J. Celotta, G. M. Whitesides, *Adv. Mater.* **1997**, *9*, 147–149.
[25] T. Serafini, T. E. Kennedy, M. J. Galko, C. Mirzayan, T. M. Jessell, M. Tessierlavigne, *Cell* **1994**, *78*, 409–424.
[26] R. Shirasaki, C. Mirzayan, M. TessierLavigne, F. Murakami, *Neuron* **1996**, *17*, 1079–1088.
[27] V. Saravia, S. Küpcü, M. Nolte, C. Huber, D. Pum, A. Fery, U. Sleytr, J. Toca-Herrera, *J. Biotech.* **2007**, *130*, 247–252.
[28] W. Senaratne, P. Sengupta, C. Harnett, H. Craighead, B. Baird, C. Ober, *J. Nanobiotechnol.* **2005**, *1*, 23–33.

Received: November 22, 2012
Revised: January 25, 2013
Published online:

DOI: 10.1002/smll.201202915